

A new channel to search for dark matter at Belle II

Jinhan Liang,^{1,2,3} Zuowei Liu,^{1,4} and Lan Yang¹

¹*Department of Physics, Nanjing University, Nanjing 210093, China*

²*Guangdong Provincial Key Laboratory of Nuclear Science, Institute of Quantum Matter, South China Normal University, Guangzhou 510006, China*

³*Guangdong-Hong Kong Joint Laboratory of Quantum Matter, Southern Nuclear Science Computing Center, South China Normal University, Guangzhou 510006, China*

⁴*CAS Center for Excellence in Particle Physics, Beijing 100049, China*

We propose a new “disappearing positron track” channel at Belle II to search for dark matter, in which a positron that is produced at the primary interaction vertex scatters with the electromagnetic calorimeter to produce dark matter particles. Such scatterings can occur via either annihilation with atomic electrons, or the bremsstrahlung process with target nuclei. The main backgrounds are due to photons and neutrons that are produced in the same scatterings and then escape detection. We require a large missing energy and further veto certain activities in the KLM detector to suppress such backgrounds. To illustrate the sensitivity of the new channel, we consider a new physics model where dark matter interacts with the standard model via a dark photon, which decays predominantly to dark matter; we find that the annihilation with atomic electrons can probe some currently unexplored parameter space.

I. INTRODUCTION

Dark matter (DM) is one of the most fundamental and longstanding problems in modern physics [1]. However, the particle property of DM remains elusive, despite the overwhelming evidence of its gravitational effects [1–4]. Particle colliders are one of the most powerful tools to search for DM. The leading DM signature studied at colliders is the so-called mono-X channel where DM are usually produced at the primary collision vertex of the collider accompanied by a standard model (SM) particle X [5–9]. Over the years, a plethora of mono-X processes have been studied, with X being photon [5, 10–12], jet [6–8, 13–15], top [16–18], bottom [19, 20], Z/W [9, 21–26], or Higgs [27–31].

In this paper, we propose a new channel to search for DM at colliders where DM are produced in collisions between SM particles and the detector, instead of at the primary collision vertex of the collider. For concreteness, in this analysis we take as an example the Belle II experiment, the electron-positron collider operated at SuperKEKB. Belle II is expected to accumulate at least 50 ab⁻¹ data and has a hermetic electromagnetic calorimeter (ECL) [32], making it an ideal machine to search for light DM as well as other new light particles [33–46].

Electrons and positrons are copiously produced at Belle II via the Bhabha scattering process, leading to $\mathcal{O}(10^{12})$ positrons expected with 50 ab⁻¹. These final state positrons can then scatter with the ECL detector to produce DM; this can occur either via the annihilation process with atomic electrons in the ECL

$$e^+ + e_A^- \rightarrow \bar{\chi} + \chi, \quad (1)$$

or via the bremsstrahlung process with target nuclei in the ECL

$$e^+ + N \rightarrow e^+ + N + \bar{\chi} + \chi, \quad (2)$$

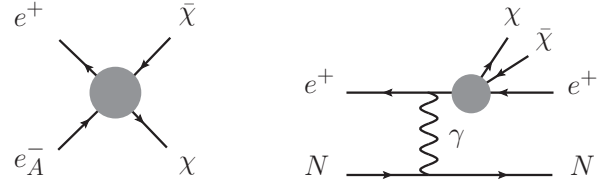


FIG. 1. Feynman diagrams of the annihilation process $e^+e_A^- \rightarrow \bar{\chi}\chi$ (left), and the bremsstrahlung process $e^+N \rightarrow e^+N\bar{\chi}\chi$ (right). The process with $\bar{\chi}\chi$ radiated from the initial state e^+ is included in the analysis, but not shown here.

where χ is the DM particle, e_A^- is the atomic electron in the ECL, and N is the target nucleus, which can be either Cs or I in the ECL. The Feynman diagrams of these two processes are shown in Fig. (1). The DM particles then escape the Belle II detectors, resulting in a missing energy signature. We note that this channel is analogous to that in electron fixed-target experiments (e.g., NA64 [47]), with the ECL detector as the target.

Unlike DM produced at the primary collision vertex, the missing energy in this new channel is preceded by a charged track in the CDC (central drift chamber) and a small amount of energy deposited in the ECL. We thus refer to this new channel as the “disappearing positron track” channel. Moreover, the disappearing positron is accompanied by an electron that has an opposite momentum to the positron track in the center of mass (CM) frame, a clear CDC track, and an energy deposition in the ECL that is consistent with the Bhabha scattering.

The collisions between positrons and the ECL can also produce photons and neutrons, which have a non-zero probability to penetrate all the sub-detectors of Belle II without leaving a trace, mimicking the signal events of DM. We find that a large missing energy in the ECL and a veto on a cluster or a track in the KLM (K_L -muon detector) [32, 46] are instrumental in controlling these

backgrounds.

To illustrate the capability of this new channel in probing DM, we consider the dark photon (DP) model in which the DP predominantly decays into DM [48]. The main results are summarized in Fig. (2). For the DP mass in the vicinity of 66 MeV, the new channel can probe unexplored parameter space, surpassing both the mono-photon channel at Belle II and the NA64 experiment.

II. DISAPPEARING POSITRON TRACK

The energy of the final state positron is measured by the ECL detector, which has a barrel region and two endcap regions. In our analysis, we only consider the positrons in the barrel region (with a polar angle between 32.2° and 128.7° in the lab frame), due to the following three reasons. First, there are less non-instrumented setups, such as magnetic wires and pole tips, between ECL and KLM in the barrel region as compared to the endcap regions [49]. This leads to a better KLM veto efficiency in the barrel region, which is essential in controlling the SM background. Second, the barrel region has a better hermiticity: Gaps between ECL crystals in the barrel region are non-projective to the collision point; however, some gaps in the endcap regions are projective so that particles can escape the ECL detector without being noticed when traversing them [50, 51]. Third, the endcap regions have more beam backgrounds [52].

Although in the signal process the positron cannot deposit all its energy in the ECL due to the production of DM, its transverse momentum can be measured in the CDC with a good resolution, e.g., $\delta p_T/p_T \simeq 0.4\%$ for $p_T \simeq 3$ GeV [53]. Using the CDC measurements (both the transverse momentum and the angular information), we can compute the positron energy, which is then required to be equal to the electron energy (measured both in the ECL and CDC) in the CM frame. To suppress the backgrounds (especially those from neutrons), we further require a large missing energy such that the final state positron only deposits at most 5% of its energy in the ECL, and veto KLM activities including multi-hits or a cluster.

III. POSITRON FLUX

Positrons at Belle II are mainly produced at the primary interaction point, via the Bhabha scattering process with the cross section [54]

$$\frac{d\sigma_B}{d\cos\theta^*} = \frac{\pi\alpha^2}{2s} \frac{(3 + \cos^2\theta^*)^2}{(1 + \cos\theta^*)^2}, \quad (3)$$

where θ^* is the polar angle of the final state positron in the CM frame, s is the square of the center of mass energy, and $\alpha \simeq 1/137$ is the fine structure constant.

Because SuperKEKB is an asymmetric collider, which collides 7 GeV electrons with 4 GeV positrons [32], the differential cross section of the Bhabha scattering in the lab frame is given by

$$\frac{d\sigma_B}{dE} = \frac{d\sigma_B}{d\cos\theta^*} \frac{\sqrt{1-\beta^2}}{\beta E^*}, \quad (4)$$

where E is the energy of the final state positron in the lab frame, $\beta = 3/11$, $E^* = \sqrt{s}/2$, and $\cos\theta^* = (\sqrt{1-\beta^2}E/E^* - 1)/\beta$. In the lab frame, the energy of the final state positron E is related to its polar angle θ via $E = E^*\sqrt{1-\beta^2}/(1-\beta\cos\theta)$. Thus, the minimum and maximum energy of the positron at the barrel region in the lab frame are $E_{\min} \simeq 4.35$ GeV (for $\theta = 128.7^\circ$) and $E_{\max} \simeq 6.62$ GeV (for $\theta = 32.2^\circ$) respectively. The total number of positrons in the barrel region is about 6×10^{11} with the total luminosity of 50 ab^{-1} .

IV. BACKGROUNDS

SM backgrounds arise when the SM particles that are produced in the collision between the final state positron and the ECL detector escape detection. Charged particles (such as electron and muon) are likely to be detected by the ECL and KLM detectors: The probability for positrons to penetrate the ECL is very small; the KLM detector, which consists of an alternating sandwich of 4.7 cm thick iron plates and active detector elements [32], is very sensitive to the muon tracks, leading to negligible muon backgrounds via the KLM veto. On the other hand, neutral particles (such as photon, neutron, and neutrino) have a significant probability to traverse the ECL and KLM detectors without being detected. Backgrounds due to neutrinos are found to be negligible, due to the large W/Z masses. Thus, the main backgrounds are due to photons and neutrons, which we discuss below.

We first discuss the photon backgrounds. Photon energy can be measured in the ECL detector, which is made up of CsI crystals with the length of $16 X_0$ [55], where $X_0 = 1.86$ cm is the radiation length of CsI [56]. The energy distribution of photons that are produced in the collision between a positron with energy E and the ECL can be well approximated by [57]

$$\frac{dN_\gamma}{dx_\gamma}(t, x_\gamma) \simeq \frac{1}{x_\gamma} \frac{(1-x_\gamma)^{(4/3)t} - e^{-(7/9)t}}{7/9 + (4/3)\ln(1-x_\gamma)}, \quad (5)$$

where $x_\gamma = E_\gamma/E$ with E_γ being the energy of the photon, and tX_0 is the position of the photon in the ECL detector. Therefore, the probability of a photon carrying more than 95% of the positron energy to escape the ECL detector is given by

$$\int_{0.95}^1 dx_\gamma \frac{dN_\gamma}{dx_\gamma}(t=16, x_\gamma) \simeq 4.7 \times 10^{-8}. \quad (6)$$

This leads to $\sim 2.8 \times 10^4$ potential background events after the ECL detector, for the 6×10^{11} positrons. Although the probability for GeV-scale photons to penetrate the whole KLM (consisting of at least 60 cm iron plates in total [32]) without producing KLM clusters is negligibly small, photons can also be absorbed by some non-instrumented setups (for example the magnet coil) between the ECL and the KLM [49]. For that reason the veto power of the KLM on photons is limited. To take into account such effects, we adopt the IFR veto efficiency at BABAR, which is about 4.5×10^{-4} [58], as the conservative estimate of the KLM veto efficiency, since the KLM veto efficiency is expected to be better than the IFR [59]. This then leads to 13 background events due to photons, for the 6×10^{11} positrons. We note in passing that if the KLM veto efficiency can be improved by one order of magnitude as compared to the IFR, the photon backgrounds will decrease to be about a single event.

We next discuss the neutron backgrounds. Neutrons with energy of several GeV are mainly produced by photo-nuclear reactions between the positron and the ECL detector [56]. To estimate such backgrounds, we simulate collisions of 10^9 positrons with 4.35 GeV energy onto a CsI target with one X_0 , by using GEANT4 (version 11.0) [60] with the FTFP_BERT physics list. Our choice of the positron energy in the simulation is motivated by the fact that $\sim 50\%$ of the positrons are in the first tenth of the entire energy range in the barrel region, according to Eq. (4). We only simulate a fraction of positrons with a thin CsI target (with one X_0) because the full simulation with a 16- X_0 CsI target is extremely time-consuming. The simulation results with the thin CsI target are acceptable for our purpose, because neutrons with significant energy are mainly produced within the first radiation length, which are confirmed in our simulations with a 2- X_0 CsI target.

To ensure that the missing energy is mainly caused by neutrons, we only select the GEANT4 simulated events that contain at least one neutron with energy exceeding 3 GeV. There are 4950 events in the 10^9 simulations that satisfy this selection cut. We then compute the total energy deposited in the ECL, by taking into account both the deposited energy in the first X_0 calculated by GEANT4, and the kinetic energy of e^\pm and γ . We further include the kinetic energy of protons with momentum less than 0.6 GeV, because such protons have a gyroradius radius $\lesssim 1.3$ m in the ECL where $B = 1.5$ T [32], and thus can deposit the kinetic energy when orbiting around. We do not add the kinetic energy of π^\pm to the deposited energy, because π^\pm decays primarily into a neutrino and a muon which deposit negligible energy to the ECL. We then require the deposited energy in the ECL to be less than 5% of the energy of the positron; there are 100 events after this detector cut. We further veto events that contain protons or π^\pm with momentum exceeding 0.6 GeV, because these charged hadrons can either deposit significant energy in the ECL and/or pro-

duce tracks in the KLM. There are 64 events after this veto.

Next we classify the remaining events according to the number of neutrons that have kinetic energy exceeding 280 MeV, the energy threshold for hadronic showers [61]. There are 13 events with a single neutron and 51 events with more than 2 neutrons. We compute the probability for a neutron to penetrate a target with length L via [62, 63]

$$P = \exp(-L/\lambda_0), \quad (7)$$

where λ_0 is the hadronic interaction length. The KLM has $\sim 3.9\lambda_0$, and the ECL has $\sim 0.8\lambda_0$ [32]. Thus, the probability for a neutron to penetrate the remaining 15 X_0 's of the ECL and the KLM is $P \simeq 0.01$. Rescaling this to the 6×10^{11} positrons, one expects ~ 81 background events due to neutrons in total.

We note that there is another source of neutrons from the beam backgrounds (dominated by 10-100 keV neutrons), which can also produce KLM hits [64] and thus complicates the situation. Because of the beam backgrounds, one cannot veto events with any hits in the KLM [49]. Fortunately, unlike neutrons with kinetic energy above 280 MeV which are expected to produce multi-hits or a cluster in the KLM, a single beam background neutron is usually absorbed in one scintillator strip [65]. For that reason, in our analysis, we only select neutrons above 280 MeV, which can be well controlled by the veto on multi-hits or a cluster in the KLM. However, since there is already a neutron with energy above 3 GeV in our selected events, including another neutron below 280 MeV would further suppress the background, leading to an even smaller neutron background. Thus, our analysis serves as a conservative estimate of the neutron backgrounds.

Taking into account backgrounds from both neutrons and photons, one expects at most ~ 94 background events for the 6×10^{11} positrons.

V. RESULT

To show the sensitivity of the “disappearing positron track” channel on DM, we consider a new physics model in which DM interacts with the SM through a DP via the Lagrangian [48]

$$\mathcal{L}_{\text{int}} = A'_\mu (eQ_f \epsilon \bar{f} \gamma^\mu f + g_\chi \bar{\chi} \gamma^\mu \chi), \quad (8)$$

where A'_μ is the DP with mass $m_{A'}$, χ is the Dirac DM with mass m_χ , f denotes the SM fermion with electric charge Q_f , e is the QED coupling, and ϵ and g_χ are coupling constants. In our analysis we fix $m_\chi = m_{A'}/3$ such that A' decays dominantly into DM in the parameter space of interest where $g_\chi \gg e\epsilon$.

We compute the signal events from both diagrams shown in Fig. (1). We first compute the annihilation

process $e^+e^- \rightarrow A' \rightarrow \chi\bar{\chi}$; the cross section is given by

$$\sigma_{\text{ann}}(\sqrt{s}) = \frac{e^2 \epsilon^2 \alpha_D}{3} \frac{s + 2m_\chi^2}{(s - m_{A'}^2)^2 + \Gamma_{A'}^2 m_{A'}^2} \sqrt{1 - \frac{4m_\chi^2}{s}}, \quad (9)$$

where $\alpha_D = g_\chi^2/4\pi$, $\Gamma_{A'}$ is the decay width of the DP, and $s = 2m_e E' + 2m_e^2 = 2m_e E_{A'}$ with E' being the energy of the positron at the collision point and $E_{A'} = E' + m_e$ being the energy of A' . Note that we have $E' \leq E$ where E is the positron energy before entering ECL. The partial decay width of the DP into DM is

$$\Gamma(A' \rightarrow \bar{\chi}\chi) = \frac{m_{A'} \alpha_D}{3} \left(1 + 2 \frac{m_\chi^2}{m_{A'}^2}\right) \sqrt{1 - \frac{4m_\chi^2}{m_{A'}^2}}. \quad (10)$$

Because the invisible decay width is much larger than the visible ones in the parameter space of interest, we use $\Gamma_{A'} \simeq \Gamma(A' \rightarrow \bar{\chi}\chi)$ in our analysis. The signal events in the annihilation process can be computed by

$$N_{\text{ann}} = \mathcal{L} \int_{E_{\text{min}}}^{E_{\text{max}}} dE \frac{d\sigma_B}{dE} \int_{0.95E}^{E+m_e} dE_{A'} \quad (11)$$

$$\times n_e T_e(E' = E_{A'} - m_e, E, L_T) \sigma_{\text{ann}}(E_{A'}),$$

where $\mathcal{L} = 50 \text{ ab}^{-1}$ is the integrated luminosity, n_e is the number density of the electron in CsI, and $d\sigma_B/dE$ is given in Eq. (4). Here $T_e(E', E, L_T)$ is the positron differential track-length distribution [57, 66–68] where $L_T = 16X_0$ is the thickness of the ECL target. The expression of T_e is given in the appendix A. The integration of $E_{A'}$ is performed for $E_{A'} > 0.95E$ so that the positron deposits less than 5% of its original energy in the ECL.

We next compute the bremsstrahlung process. In the parameter space of interest, the signal is dominated by the on-shell produced A' . Thus, the signal events are given by

$$N_{\text{bre}} = \mathcal{L} \int_{E_{\text{min}}}^{E_{\text{max}}} dE \frac{d\sigma_B}{dE} \int_{0.95E}^{E-m_e} dE_{A'} \quad (12)$$

$$\int_{E_{A'}}^E dE' n_N T_e(E', E, X_0) \frac{d\sigma_{\text{bre}}}{dE_{A'}},$$

where n_N is the number density of I (or Cs). Here $d\sigma_{\text{bre}}/dE_{A'}$ is the differential cross section of the on-shell produced A' [69–71],

$$\frac{d\sigma_{\text{bre}}}{dE_{A'}} = (\phi_I + \phi_{\text{Cs}}) \frac{4\alpha^3 \epsilon^2}{E'} \frac{x(1-x+x^2/3)}{m_{A'}^2(1-x) + m_e^2 x^2}, \quad (13)$$

where $x \equiv E_{A'}/E'$, and ϕ_N denotes the effective flux of photons from nucleus N [69]:

$$\phi_N = \int_{t_{\text{min}}}^{t_{\text{max}}} dt \frac{t - t_{\text{min}}}{t^2} \left[\frac{Za^2 t}{(1+a^2 t)(1+t/d)} \right]^2, \quad (14)$$

with $t_{\text{min}} = (m_{A'}^2/2E')^2$, $t_{\text{max}} = m_{A'}^2 + m_e^2$, $a = 111m_e^{-1}Z^{-1/3}$, and $d = 0.164A^{-2/3} \text{ GeV}^2$. We use

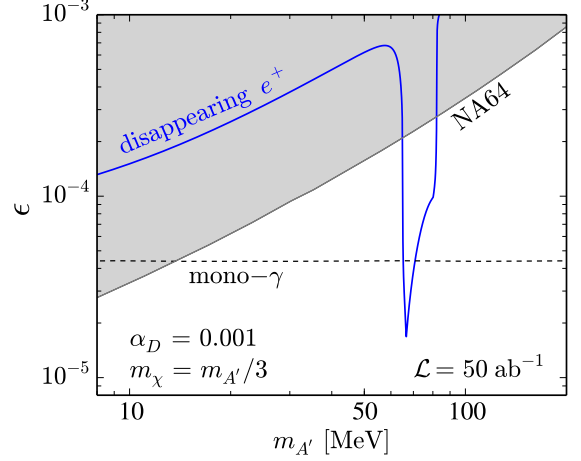


FIG. 2. Belle II sensitivity on ϵ with 50 ab^{-1} integrated luminosity as a function of the DP mass $m_{A'}$ from the “disappearing positron track” (blue solid). Here we fix $\alpha_D = 0.001$ and $m_\chi = m_{A'}/3$. Belle II sensitivity from the mono-photon channel with 50 ab^{-1} (gray dashed) is rescaled from the result with 20 fb^{-1} in Ref. [32]. The NA64 constraints (gray shaded region) [72] with 2.84×10^{11} electrons on target are also shown.

$Z = 53$ (55) and $A = 127$ (133) for I (Cs). Here we only consider the dominant elastic form factor.

Fig. (2) shows the expected 90% CL limits on ϵ from the “disappearing positron track” channel, as a function of the DP mass, where we take $m_{A'} = 3m_\chi$, $\mathcal{L} = 50 \text{ ab}^{-1}$, and $\alpha_D = 0.001$. We compute the 90% CL limits by using $N_s/\sqrt{N_b} = \sqrt{2.71}$ [45] where $N_s = N_{\text{ann}} + N_{\text{bre}}$ and $N_b = 94$. We find that in the narrow mass window, $66 \text{ MeV} \lesssim m_{A'} \lesssim 82 \text{ MeV}$, the annihilation process with the atomic electrons dominates; outside this region, the bremsstrahlung process dominates. The DP models can also be searched for in the mono-photon channel $e^+e^- \rightarrow \gamma A'$ at Belle II [32] and by the missing energy signature at NA64 [72]. We find that the best limit on ϵ from the new “disappearing positron track” channel is $\epsilon \lesssim 1.7 \times 10^{-5}$, which occurs in the vicinity of $m_{A'} = 66 \text{ MeV}$, surpassing both the mono-photon channel at Belle II and the NA64 constraints [72].

VI. SUMMARY

In this paper, we propose a new “disappearing positron track” channel at Belle II to search for DM, where DM are generated via collisions between positrons and the ECL. The major backgrounds are due to photons and neutrons produced in the same collisions. We design a set of detector cuts to reconstruct such a new signal from the Belle II data, as well as to suppress various SM backgrounds. We compute the sensitivity of the new channel on the invisible dark photon model. We find that the new channel at Belle II can probe $\epsilon \simeq 1.7 \times 10^{-5}$ with

50 ab^{-1} data for dark photon mass at ~ 66.66 MeV, surpassing both the mono-photon channel at Belle II and the missing energy channel at NA64.

ACKNOWLEDGMENTS

We thank Luigi Corona, Torben Ferber, and Li-Gang Xia for correspondence and discussions. The work is supported in part by the National Natural Science Foundation of China under Grant Nos. 12275128 and 12147103, by the Science and Technology Program of Guangzhou No. 2019050001, and by the Guangdong Major Project of Basic and Applied Basic Research No. 2020B0301030008.

Appendix A: Track length

In this appendix we provide the expression of the differential track-length distribution for positrons used in our analysis. For positrons with initial energy E to enter a target with thickness L_T , the differential track-length distribution as a function of the positron energy E' can

be computed by [67, 68]

$$T_e(E', E, L_T) = X_0 \int_0^{L_T/X_0} I_e(E', E, t) dt, \quad (\text{A1})$$

where X_0 is the radiation length of the target. Here $I_e(E', E, t)$ is the energy distribution of E' at the depth tX_0 , which can be computed iteratively such that $I_e = \sum_i I_e^{(i)}$ where $I_e^{(i)}$ denotes the i -th generation positrons [57]. We adopt the analytical model of Ref. [57] up to second-generation positrons, which are found to be in good agreement with simulations in Ref. [67]. The contributions from the first two generations are [57]

$$I_e^{(1)}(E', E, t) = \frac{1}{E} \frac{(\ln(1/v))^{b_1 t - 1}}{\Gamma(b_1 t)}, \quad (\text{A2})$$

$$I_e^{(2)}(E', E, t) = \frac{2}{E} \int_v^1 \frac{dx}{x^2} \frac{1}{b_2 + b_1 \ln(1-x)} \times \left[\frac{(1-x)^{b_1 t} - (1-v/x)^{b_1 t}}{b_1 \ln[(x-x^2)/(x-v)]} + \frac{e^{-b_2 t} - (1-v/x)^{b_1 t}}{b_2 + b_1 \ln(1-v/x)} \right], \quad (\text{A3})$$

where $b_1 = 4/3$, $b_2 = 7/9$, $v = E'/E$.

-
- [1] G. Bertone and D. Hooper, “History of dark matter,” *Rev. Mod. Phys.* **90** (2018) 045002 [[arXiv:1605.04909](#)].
 - [2] J. Alexander *et al.*, “Dark Sectors 2016 Workshop: Community Report.” [arXiv:1608.08632](#).
 - [3] M. Battaglieri *et al.*, “US Cosmic Visions: New Ideas in Dark Matter 2017: Community Report.” [arXiv:1707.04591](#).
 - [4] A. Arbey and F. Mahmoudi, “Dark matter and the early Universe: a review,” *Prog. Part. Nucl. Phys.* **119** (2021) 103865 [[arXiv:2104.11488](#)].
 - [5] A. Birkedal, K. Matchev, and M. Perelstein, “Dark matter at colliders: A Model independent approach,” *Phys. Rev. D* **70** (2004) 077701 [[hep-ph/0403004](#)].
 - [6] J. L. Feng, S. Su, and F. Takayama, “Lower limit on dark matter production at the large hadron collider,” *Phys. Rev. Lett.* **96** (2006) 151802 [[hep-ph/0503117](#)].
 - [7] M. Beltran, D. Hooper, E. W. Kolb, Z. A. C. Krusberg, and T. M. P. Tait, “Maverick dark matter at colliders,” *JHEP* **09** (2010) 037 [[arXiv:1002.4137](#)].
 - [8] Y. Bai, P. J. Fox, and R. Harnik, “The Tevatron at the Frontier of Dark Matter Direct Detection,” *JHEP* **12** (2010) 048 [[arXiv:1005.3797](#)].
 - [9] F. J. Petriello, S. Quackenbush, and K. M. Zurek, “The Invisible Z' at the CERN LHC,” *Phys. Rev. D* **77** (2008) 115020 [[arXiv:0803.4005](#)].
 - [10] P. J. Fox, R. Harnik, J. Kopp, and Y. Tsai, “LEP Shines Light on Dark Matter,” *Phys. Rev. D* **84** (2011) 014028 [[arXiv:1103.0240](#)].
 - [11] Y. Gershtein, F. Petriello, S. Quackenbush, and K. M. Zurek, “Discovering hidden sectors with mono-photon Z' searches,” *Phys. Rev. D* **78** (2008) 095002 [[arXiv:0809.2849](#)].
 - [12] W. Abdallah, J. Fiaschi, S. Khalil, and S. Moretti, “Mono-jet, -photon and -Z signals of a supersymmetric (B – L) model at the Large Hadron Collider,” *JHEP* **02** (2016) 157 [[arXiv:1510.06475](#)].
 - [13] P. J. Fox, R. Harnik, J. Kopp, and Y. Tsai, “Missing Energy Signatures of Dark Matter at the LHC,” *Phys. Rev. D* **85** (2012) 056011 [[arXiv:1109.4398](#)].
 - [14] A. Rajaraman, W. Shepherd, T. M. P. Tait, and A. M. Wijangco, “LHC Bounds on Interactions of Dark Matter,” *Phys. Rev. D* **84** (2011) 095013 [[arXiv:1108.1196](#)].
 - [15] M. Papucci, A. Vichi, and K. M. Zurek, “Monojet versus the rest of the world I: t-channel models,” *JHEP* **11** (2014) 024 [[arXiv:1402.2285](#)].
 - [16] J. Andrea, B. Fuks, and F. Maltoni, “Monotops at the LHC,” *Phys. Rev. D* **84** (2011) 074025 [[arXiv:1106.6199](#)].
 - [17] J.-L. Agram, J. Andrea, M. Buttignol, E. Conte, and B. Fuks, “Monotop phenomenology at the Large Hadron Collider,” *Phys. Rev. D* **89** (2014) 014028 [[arXiv:1311.6478](#)].
 - [18] I. Boucheneb, G. Cacciapaglia, A. Deandrea, and B. Fuks, “Revisiting monotop production at the LHC,” *JHEP* **01** (2015) 017 [[arXiv:1407.7529](#)].
 - [19] T. Lin, E. W. Kolb, and L.-T. Wang, “Probing dark matter couplings to top and bottom quarks at the LHC,” *Phys. Rev. D* **88** (2013) 063510 [[arXiv:1303.6638](#)].
 - [20] E. Izaguirre, G. Krnjaic, and B. Shuve, “The Galactic Center Excess from the Bottom Up,” *Phys. Rev. D* **90** (2014) 055002 [[arXiv:1404.2018](#)].

- [21] L. M. Carpenter, A. Nelson, C. Shimmin, T. M. P. Tait, and D. Whiteson, “Collider searches for dark matter in events with a Z boson and missing energy,” *Phys. Rev. D* **87** (2013) 074005 [[arXiv:1212.3352](#)].
- [22] N. F. Bell, *et al.*, “Searching for Dark Matter at the LHC with a Mono-Z,” *Phys. Rev. D* **86** (2012) 096011 [[arXiv:1209.0231](#)].
- [23] N. F. Bell, Y. Cai, and R. K. Leane, “Mono-W Dark Matter Signals at the LHC: Simplified Model Analysis,” *JCAP* **01** (2016) 051 [[arXiv:1512.00476](#)].
- [24] N. F. Bell, Y. Cai, J. B. Dent, R. K. Leane, and T. J. Weiler, “Dark matter at the LHC: Effective field theories and gauge invariance,” *Phys. Rev. D* **92** (2015) 053008 [[arXiv:1503.07874](#)].
- [25] U. Haisch, F. Kahlhoefer, and T. M. P. Tait, “On Mono-W Signatures in Spin-1 Simplified Models,” *Phys. Lett. B* **760** (2016) 207–213 [[arXiv:1603.01267](#)].
- [26] Y. Bai and T. M. P. Tait, “Searches with Mono-Leptons,” *Phys. Lett. B* **723** (2013) 384–387 [[arXiv:1208.4361](#)].
- [27] A. A. Petrov and W. Shepherd, “Searching for dark matter at LHC with Mono-Higgs production,” *Phys. Lett. B* **730** (2014) 178–183 [[arXiv:1311.1511](#)].
- [28] L. Carpenter, *et al.*, “Mono-Higgs-boson: A new collider probe of dark matter,” *Phys. Rev. D* **89** (2014) 075017 [[arXiv:1312.2592](#)].
- [29] A. Berlin, T. Lin, and L.-T. Wang, “Mono-Higgs Detection of Dark Matter at the LHC,” *JHEP* **06** (2014) 078 [[arXiv:1402.7074](#)].
- [30] K. Ghorbani and L. Khalkhali, “Mono-Higgs signature in a fermionic dark matter model,” *J. Phys. G* **44** (2017) 105004 [[arXiv:1608.04559](#)].
- [31] J. M. No, “Looking through the pseudoscalar portal into dark matter: Novel mono-Higgs and mono-Z signatures at the LHC,” *Phys. Rev. D* **93** (2016) 031701 [[arXiv:1509.01110](#)].
- [32] E. Kou and P. Urquijo, eds., “The Belle II Physics Book,” *PTEP* **2019** (2019) 123C01 [[arXiv:1808.10567](#)]. [Erratum: *PTEP* 2020, 029201 (2020)].
- [33] T. Hauth, “Search for dark matter and dark sector at Belle II,” *PoS HQL2018* (2018) 060.
- [34] J. Liang, Z. Liu, Y. Ma, and Y. Zhang, “Millicharged particles at electron colliders,” *Phys. Rev. D* **102** (2020) 015002 [[arXiv:1909.06847](#)].
- [35] T. Araki, S. Hoshino, T. Ota, J. Sato, and T. Shimomura, “Detecting the $L_\mu - L_\tau$ gauge boson at Belle II,” *Phys. Rev. D* **95** (2017) 055006 [[arXiv:1702.01497](#)].
- [36] Y. Zhang, *et al.*, “Probing the $L_\mu - L_\tau$ gauge boson at electron colliders,” *Phys. Rev. D* **103** (2021) 015008 [[arXiv:2012.10893](#)].
- [37] D. W. Kang, P. Ko, and C.-T. Lu, “Exploring properties of long-lived particles in inelastic dark matter models at Belle II,” *JHEP* **04** (2021) 269 [[arXiv:2101.02503](#)].
- [38] M. Duerr, *et al.*, “Invisible and displaced dark matter signatures at Belle II,” *JHEP* **02** (2020) 039 [[arXiv:1911.03176](#)].
- [39] M. Duerr, T. Ferber, C. Garcia-Cely, C. Hearty, and K. Schmidt-Hoberg, “Long-lived Dark Higgs and Inelastic Dark Matter at Belle II,” *JHEP* **04** (2021) 146 [[arXiv:2012.08595](#)].
- [40] T. Ferber, C. Garcia-Cely, and K. Schmidt-Hoberg, “Belle II sensitivity to long-lived dark photons.” [arXiv:2202.03452](#).
- [41] **Belle-II** Collaboration, “Search for Axion-Like Particles produced in e^+e^- collisions at Belle II,” *Phys. Rev. Lett.* **125** (2020) 161806 [[arXiv:2007.13071](#)].
- [42] E. Izaguirre, T. Lin, and B. Shuve, “Searching for Axionlike Particles in Flavor-Changing Neutral Current Processes,” *Phys. Rev. Lett.* **118** (2017) 111802 [[arXiv:1611.09355](#)].
- [43] Y. Jho, Y. Kwon, S. C. Park, and P.-Y. Tseng, “Search for muon-philic new light gauge boson at Belle II,” *JHEP* **10** (2019) 168 [[arXiv:1904.13053](#)].
- [44] **Belle-II** Collaboration, “Search for an Invisibly Decaying Z' Boson at Belle II in $e^+e^- \rightarrow \mu^+\mu^-(e^\pm\mu^\mp)$ Plus Missing Energy Final States,” *Phys. Rev. Lett.* **124** (2020) 141801 [[arXiv:1912.11276](#)].
- [45] J. Liang, Z. Liu, and L. Yang, “Probing sub-GeV leptophilic dark matter at Belle II and NA64,” *JHEP* **05** (2022) 184 [[arXiv:2111.15533](#)].
- [46] M. J. Dolan, T. Ferber, C. Hearty, F. Kahlhoefer, and K. Schmidt-Hoberg, “Revised constraints and Belle II sensitivity for visible and invisible axion-like particles,” *JHEP* **12** (2017) 094 [[arXiv:1709.00009](#)]. [Erratum: *JHEP* 03, 190 (2021)].
- [47] Y. M. Andreev *et al.*, “Improved exclusion limit for light dark matter from e^+e^- annihilation in NA64,” *Phys. Rev. D* **104** (2021) L091701 [[arXiv:2108.04195](#)].
- [48] M. Fabbrichesi, E. Gabrielli, and G. Lanfranchi, “The Dark Photon.” [arXiv:2005.01515](#).
- [49] Torben Ferber, private communication.
- [50] C. Hearty. https://indico.fnal.gov/event/13702/contributions/21158/attachments/13740/17506/Dark_sector_BaBar_Belle_II_Hearty.pdf.
- [51] **Belle** Collaboration, “The Belle Detector,” *Nucl. Instrum. Meth. A* **479** (2002) 117–232.
- [52] S. R. de Jong, *Study of Thermal Neutron Flux from SuperKEKB in the Belle II Commissioning Detector*. PhD thesis, Victoria U., 2017.
- [53] T. V. Dong, *et al.*, “Calibration and alignment of the Belle II central drift chamber,” *Nucl. Instrum. Meth. A* **930** (2019) 132–141.
- [54] M. E. Peskin and D. V. Schroeder, *An Introduction to quantum field theory*. Addison-Wesley, Reading, USA, 1995.
- [55] **BELLE II calorimeter Group** Collaboration, “Electromagnetic calorimeter of the Belle II detector,” *J. Phys. Conf. Ser.* **928** (2017) 012021.
- [56] **Particle Data Group** Collaboration, “Review of Particle Physics,” *Phys. Rev. D* **98** (2018) 030001.
- [57] Y.-S. Tsai and V. Whitis, “THICK TARGET BREMSSTRAHLUNG AND TARGET CONSIDERATION FOR SECONDARY PARTICLE PRODUCTION BY ELECTRONS,” *Phys. Rev.* **149** (1966) 1248–1257.
- [58] **BaBar** Collaboration in *34th International Conference on High Energy Physics*. 2008. [arXiv:0808.0017](#).
- [59] Luigi Corona, private communication.
- [60] **GEANT4** Collaboration, “GEANT4—a simulation toolkit,” *Nucl. Instrum. Meth. A* **506** (2003) 250–303.
- [61] L. Cerrito, *Radiation and Detectors: Introduction to the Physics of Radiation and Detection Devices*. Graduate Texts in Physics. Springer, 2017.
- [62] C. Grupen and B. Schwartz, *Particle detectors*. Cambridge Univ. Pr., Cambridge, UK, 2008.

- [63] S. Andreas *et al.*, “Proposal for an Experiment to Search for Light Dark Matter at the SPS.” [arXiv:1312.3309](#).
- [64] **Belle-II** Collaboration, “Belle II Technical Design Report.” [arXiv:1011.0352](#).
- [65] T. Aushev *et al.*, “A scintillator based endcap K_L and muon detector for the Belle II experiment,” *Nucl. Instrum. Meth. A* **789** (2015) 134–142 [[arXiv:1406.3267](#)].
- [66] J. D. Bjorken, *et al.*, “Search for Neutral Metastable Penetrating Particles Produced in the SLAC Beam Dump,” *Phys. Rev. D* **38** (1988) 3375.
- [67] L. Marsicano, *et al.*, “Dark photon production through positron annihilation in beam-dump experiments,” *Phys. Rev. D* **98** (2018) 015031 [[arXiv:1802.03794](#)].
- [68] L. Marsicano, *et al.*, “Novel Way to Search for Light Dark Matter in Lepton Beam-Dump Experiments,” *Phys. Rev. Lett.* **121** (2018) 041802 [[arXiv:1807.05884](#)].
- [69] J. D. Bjorken, R. Essig, P. Schuster, and N. Toro, “New Fixed-Target Experiments to Search for Dark Gauge Forces,” *Phys. Rev. D* **80** (2009) 075018 [[arXiv:0906.0580](#)].
- [70] S. N. Gninenko, D. V. Kirpichnikov, M. M. Kirsanov, and N. V. Krasnikov, “The exact tree-level calculation of the dark photon production in high-energy electron scattering at the CERN SPS,” *Phys. Lett. B* **782** (2018) 406–411 [[arXiv:1712.05706](#)].
- [71] Y.-S. Liu and G. A. Miller, “Validity of the Weizsäcker-Williams approximation and the analysis of beam dump experiments: Production of an axion, a dark photon, or a new axial-vector boson,” *Phys. Rev. D* **96** (2017) 016004 [[arXiv:1705.01633](#)].
- [72] D. Banerjee *et al.*, “Dark matter search in missing energy events with NA64,” *Phys. Rev. Lett.* **123** (2019) 121801 [[arXiv:1906.00176](#)].